GA–A23816

THE QUIESCENT DOUBLE BARRIER REGIME IN DIII–D

by
C.M. GREENFIELD, K.H. BURRELL, E.J. DOYLE, R.J. GROEBNER, W.P. WEST, T.A. CASPER, J.C. DeBOO, C. FENZI, P. GOHIL, J.E. KINSEY, L.L. LAO, J.N. LEBOEUF, M.A. MAKOWSKI, G.R. McKEE, R.A. MOYER, M. MURAKAMI, R.I. PINSKER, G.D. PORTER, C.L. RETTIG, T.L. RHODES, G.M. STAEBLER, B.W. STALLARD, E.J. SYNAKOWSKI, L. ZENG, and The DIII–D TEAM

NOVEMBER 2001

DISCLAIMER

This report was prepared as an account of work sponsored by an agency of the United States Government. Neither the United States Government nor any agency thereof, nor any of their employees, makes any warranty, express or implied, or assumes any legal liability or responsibility for the accuracy, completeness, or usefulness of any information, apparatus, product, or process disclosed, or represents that its use would not infringe privately owned rights. Reference herein to any specific commercial product, process, or service by trade name, trademark, manufacturer, or otherwise, does not necessarily constitute or imply its endorsement, recommendation, or favoring by the United States Government or any agency thereof. The views and opinions of authors expressed herein do not necessarily state or reflect those of the United States Government or any agency thereof.

GA–A23816

THE QUIESCENT DOUBLE BARRIER REGIME IN DIII–D

by
C.M. GREENFIELD, K.H. BURRELL, E.J. DOYLE,[*] R.J. GROEBNER, W.P. WEST, T.A. CASPER,[†] J.C. DeBOO, C. FENZI,[‡] P. GOHIL, J.E. KINSEY,[§] L.L. LAO, J.N. LEBOEUF,[¶] M.A. MAKOWSKI,[†] G.R. McKEE,[‡] R.A. MOYER,[¶] M. MURAKAMI[△] R.I. PINSKER, G.D. PORTER,[†] C.L. RETTIG,[*] T.L. RHODES,[*] G.M. STAEBLER, B.W. STALLARD,[†] E.J. SYNAKOWSKI,[#] L. ZENG,[*] and The DIII–D TEAM

This is a preprint of a paper to be presented at the 8th IAEA Technical Committee Meeting on H–Mode Physics and Transport Barriers, Toki, Japan, September 5–7, 2001, and to be published in the *Plasma Physics and Controlled Fusion.*

[*]University of California, Los Angeles, California.
[†]Lawrence Livermore National Laboratory, Livermore, California.
[‡]University of Wisconsin, Madison, Wisconsin.
[§]Lehigh University, Bethlehem, Pennsylvania.
[¶]University of California, San Dlego, California.
[△]Oak Ridge National Laboratory, Oak Ridge, Tennessee.
[#]Princeton Plasma Physics Laboratory, Princeton, New Jersey.

Work supported by
the U.S. Department of Energy under Contract Nos. DE-AC03-99ER54463, W-7405-ENG-48, DE-AC05-00OR22725, DE-AC02-76CH03073 and Grant Nos. DE-FG03-01ER54615, DE-FG03-96ER54373, DE-FG03-95ER54294, DE-FG02-92ER54141 and DE-FG03-95ER54294

GENERAL ATOMICS PROJECT 30033
NOVEMBER 2001

ABSTRACT

The Quiescent Double Barrier (QDB) regime is a high performance regime recently identified in DIII–D and characterized by a double transport barrier structure (core and edge) that can be maintained for several seconds, often limited only by the pulse length capabilities of the DIII–D hardware. The QDB regime has been sustained for up to 25 τ_E with fusion performance of up to $\beta_N H_{89} \approx 7$. The edge barrier is ELM-free, but modulated by low frequency MHD activity that allows density control via an external cryopump. The core barrier is similar to those seen in previous internal transport barrier experiments, but is maintained without complete stabilization of turbulence. Instead, the turbulence correlation lengths become very short so as to minimize the transport length scales. The two barriers are separated by a region of high transport that is a consequence of a zero crossing in the $E \times B$ shearing rate. These discharges typically possess highly peaked density profiles. This has several implications: narrow bootstrap current profile, reduced beta limit and increased impurity retention. We will report on studies of each of these issues.

1. INTRODUCTION

For several years, experiments in many tokamak devices have focused on regimes with internal transport barriers (ITB) as candidates for further Advanced Tokamak development [1–5]. These regimes often lead to peaked pressure profiles and have inherently low global β limits, and are difficult to sustain. For an even longer time, the H–mode [6], with transport barriers near the plasma boundary, has been studied and has become the default scenario for next-step devices. There is an obvious attraction to combining these regimes, but our ability to produce such regimes, with their inherent improved MHD stability [7] and bootstrap current alignment [8] characteristics, has so far been limited. Although ELMing H–mode regimes have been combined with an ITB, this usually occurs with some degradation to the ITB due presumably to ELM coupling [9]. ELM-free H–modes have also been combined with an ITB, but this results in merging of the core and edge barriers and ultimately to MHD termination of the high performance regime [10,11].

Recent experiments in counter neutral beam injected (counter-NBI) discharges in DIII–D have produced a new regime with combined edge and core barriers, the Quiescent Double Barrier (QDB) regime [12–14]. This regime obtains the same advantages as an ELMing H–mode regime with a core barrier, but without some of the costs: the core barrier is allowed to form and be sustained with no evidence of deterioration. The H–mode edge is ELM-free, but not in the traditional sense. In these discharges, low frequency, sustained MHD oscillations replace the ELMs in the role of increasing particle transport near the boundary to allow particle control via an external cryopump. In most cases, these oscillations take the form of the Edge Harmonic Oscillation, a low-*n* oscillation localized at or slightly outside the boundary [13]. In a few cases, a global MHD mode with a significant component near the edge has been observed to produce results almost identical to those with the EHO. The core barrier is similar to those seen with an L–mode edge, with no obvious signs of deterioration. A remarkable result is that these barriers seem to exist without complete stabilization of long wavelength turbulence. Rather, in these discharges, the turbulence correlation lengths become very small, thereby reducing the spatial scale of the transport rather than the amplitude of the turbulence.

Discharges operated in the QDB regime have exhibited sustained fusion performance of $\beta_N H_{89} \approx 7$ for up to 10 τ_E and up to 25 τ_E for >3.5 s with somewhat lower performance. The duration of these discharges is often limited only by the available neutral beam pulse length.

In this paper, we will first discuss the global behavior of the QDB regime, including the conditions for producing it. We will then summarize the behavior of the edge region; a more detailed description is available in Ref. [15]. The behavior of the core region will be discussed, covering both transport and MHD stability. Finally, we will summarize the results.

2. GLOBAL BEHAVIOR

The QDB regime has so far only been obtained in counter-NBI heated discharges in DIII–D. These discharges are operated similarly to previous experiments where we produced an ITB with an L–mode edge [16], except that the plasma configuration has been changed from a high-field-side limiter to a single-null divertor, with both divertor legs being coupled to divertor cryopumps. The pumping is an important ingredient, as the QDB regime is accessed at low densities $\left(n_e^{pedestal} \approx 1\text{–}2\times10^{19}\ m^{-3}\right)$.

This results in a rapid transition to a low-density ELMing H–mode after heating power is applied. In many discharges, particularly those with higher heating power, a series of rapid locked modes occurs during this phase. This usually has the effect of reducing the q profile, but in many cases, the plasma can recover and obtain a QDB regime with full performance. We have had some success controlling these locked modes using error field reduction techniques [17], but it is difficult due to the extremely rapid onset of these events.

After several hundred milliseconds, the ELMs spontaneously cease, being replaced in most cases by the EHO. This phase is critical: if the EHO or another MHD oscillation with similar impact on the edge characteristics is obtained [15], the ITB forms spontaneously in nearly all cases with sufficient heating power. If not, the plasma will usually remain in an ELMing H–mode state for the remainder of the discharge.

In most cases, there is no obvious power threshold. In the conditions where most QDB experiments have been performed (I_p = –1.3 MA, B_T = 1.8-2.1 T, q_{95} = 3.5–4.5), the EHO and subsequent ITB appear at any power level where the L–H transition occurs. The height and spatial extent of the ITB varies strongly with the power, while that of the edge barrier is less sensitive. At higher plasma current (1.6 MA), we begin to observe evidence of a power threshold for the EHO at around 10–12 MW. It should be noted that these discharges were created with a slightly different, squarer, shape, and we cannot definitively associate the appearance of the threshold with either current or shape alone.

During the ELM-free phase, which can last several seconds, most of the characteristics of the plasma, including density, fusion reaction rate and radiated power, become steady (Fig. 1). Although the safety factor q continues to evolve, this evolution is usually very slow, owing to the counter-neutral beam current drive (counter-NBCD) which assists in maintaining an elevated q profile. As will be discussed later, this is believed to be an ideal target for demonstration of ECCD to bring the current profile to a steady-state. Such experiments are anticipated for the near future.

Once the QDB regime is entered, provision of additional heating power can increase fusion performance. Although detailed studies of global confinement dependencies have not yet been undertaken, the data obtained so far seem to indicate little or no confinement degradation. In the discharges completed so far, a beta limit appears to exist at about $\beta_N \approx 3$. Attempts to exceed this level can result in either disruption or just loss of the QDB regime, usually followed by a return to ELMing H–mode.

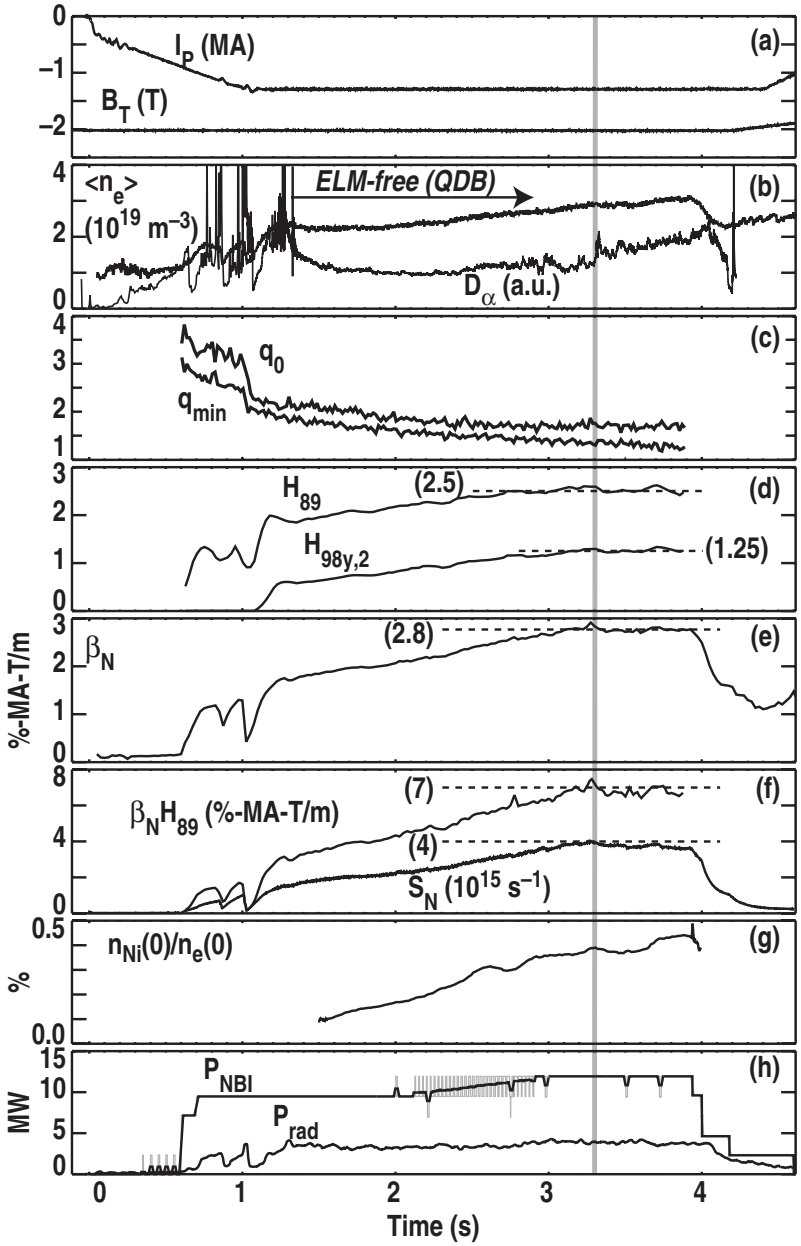

Fig. 1. Time history of a QDB discharge, showing (a) plasma current and toroidal field, (b) density and D_α, (c) q_0 and q_{min}, (d) H_{89} and $H_{98y,2}$ (e) β_N, (f) $\beta_N H_{89}$ and neutron rate, (g) central nickel impurity concentration, (h) heating and radiated power (103740).

3. EDGE TRANSPORT BARRIER

The Quiescent Double Barrier regime is an ELM-free regime, but not in the usual sense. In these discharges, the edge region is dominated by low to moderate n (n = 1–10) MHD activity (Fig. 2). In most cases, this takes the form of the Edge Harmonic Oscillation (EHO), which is highly localized near or slightly outside the separatrix. A more complete description of the characteristics of the EHO is given in a separate paper [15].

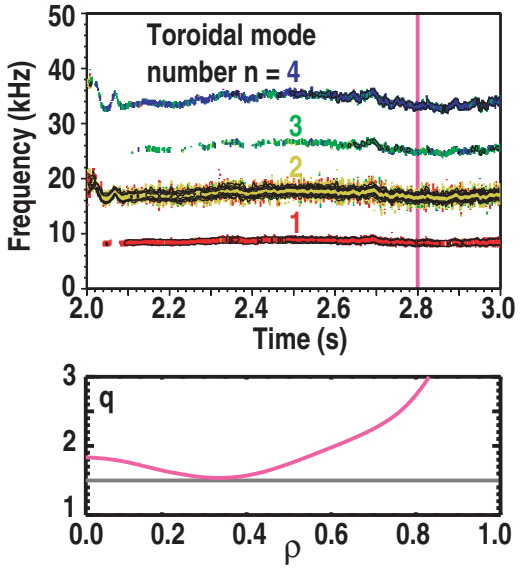

Fig. 2. (a) Intensity contours of the EHO at different toroidal mode numbers from magnetic measurements. (b) q profile as a function of ρ, the square root of the normalized toroidal flux at the time shown by a vertical bar in (a) (106919).

The EHO has the effect of increasing particle transport near the boundary, thus facilitating particle control via an external cryopump. It does not, however, cause some of the less desirable effects of ELMs. In particular, unlike ELMs, the effect of the EHO is highly localized and does not perturb the interior of the plasma. Therefore, the ITB is allowed to develop undisturbed by activity propagating from the edge.

In a few cases, the QDB regime has been obtained without the EHO. This occurs after a locked mode during the current ramp results in $q_{\min}$ being reduced to near unity before the formation of the ITB. In such cases, a global MHD mode appears with a significant edge component. The exact nature of this mode has not yet been identified, but it

generally appears with n=1 and with a somewhat higher frequency than the EHO (Fig. 3). This results in a set of profiles that are indistinguishable from the QDB with an EHO. So, the EHO is not a unique requirement for formation of a QDB discharge, but some sort of MHD activity near the edge is required for density control.

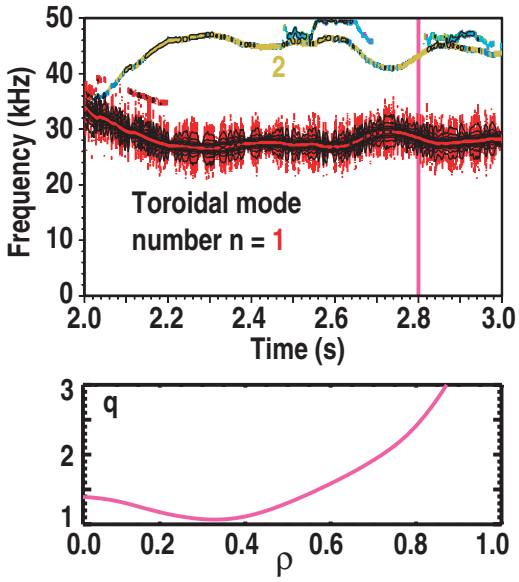

Fig. 3. (a) Intensity contours of global MHD activity from magnetic measurements. (b) q profile at the time shown by a vertical bar in (a) (106956).

The core and edge barriers are insulated from each other by virtue of a zero crossing in the $E \times B$ shearing rate (Fig. 4) $\omega_{E\times B}$. Here, the radial electric field E_r is calculated using the force balance equation:

$$E_r = \left(Z_i e n_i\right)^{-1} \nabla p_i - v_{\theta i} B_\phi + v_{\phi i} B_\theta \quad , \tag{1}$$

where i can denote any ion species, but here refers to the carbon impurity measured by charge exchange recombination. E_r is strongly negative in the core, a consequence of the dominant pressure gradient term in counter- or balanced-NBI discharges. As in other H–modes, it is also strongly negative near the edge. Connecting these regions is a flattened region.

The $E \times B$ shearing rate is calculated according to Ref. [18]:

$$\omega_{E\times B} = \frac{\left(RB_\theta\right)^2}{B} \frac{\partial}{\partial \psi} \left(\frac{E_r}{RB_\theta} \right) \quad . \tag{2}$$

Both simulated [19] and experimental [1,2,10,16] observations indicate that a large amplitude of $\omega_{E\times B}$ is stabilizing to low-k drift ballooning modes. The zero crossing in $\omega_{E\times B}$ at $\rho \approx 0.88$, a consequence of the flattened region in the E_r profile, locally facilitates a region of high transport that prevents the two barriers from merging. Note that although our experience suggests that merging the two barriers can result in very high fusion performance [10], this also has resulted in a highly transient regime [11]. This separation may be an essential factor in allowing this regime to become nearly steady.

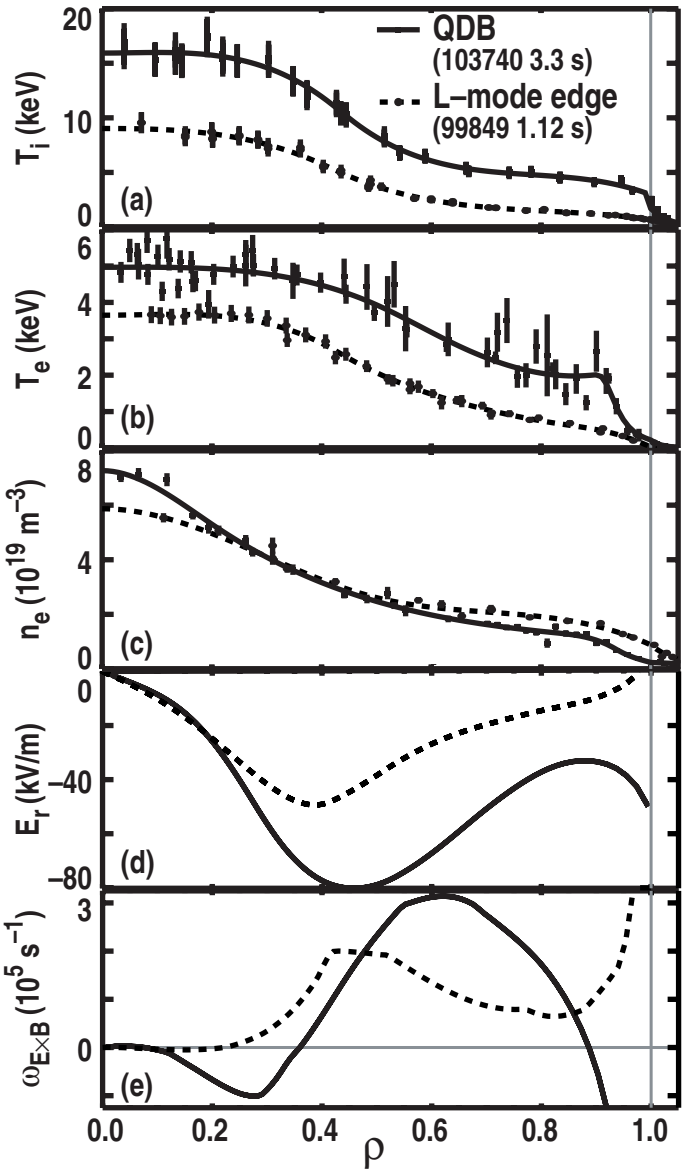

Fig. 4. Kinetic profiles from a QDB (103740) and ITB with an L–mode edge (99849). (a) Ion and (b) electron temperatures, (c) electron density, (d) radial electric field and (e) $E \times B$ shearing rate.

4. CORE BARRIER

The core barrier region of the QDB discharges is similar in many ways to those seen in previous discharges with an L–mode edge [16]. The most important difference is that an edge pedestal, which can, in many cases, become quite large, elevates the temperature profiles (Fig. 4). The density profile is also different: even though these discharges maintain an H–mode edge, the pedestal density is lower than that seen in the similar L–mode discharge. This is because unlike the L–mode discharges, which were operated in a limiter configuration, these discharges are operated with a divertor configuration where both divertor legs are strongly pumped. The density profiles in these discharges can also become quite peaked. This peakedness has some disadvantages, which are discussed below.

An interesting feature of these ITBs is that they exist with only incomplete suppression of turbulence. Typical ITBs in DIII–D form where the $E \times B$ shearing rate increases to become larger than the growth rate calculated for low-k drift-ballooning modes. In these cases, fluctuation measurements typically indicate that the amplitude of the local turbulence is decreased to at or below the detection limit. This is not the case for many QDB discharges. FIR scattering indicates that the broadband turbulence observed during the entry to the QDB regime remains fairly large in amplitude (Fig. 5).

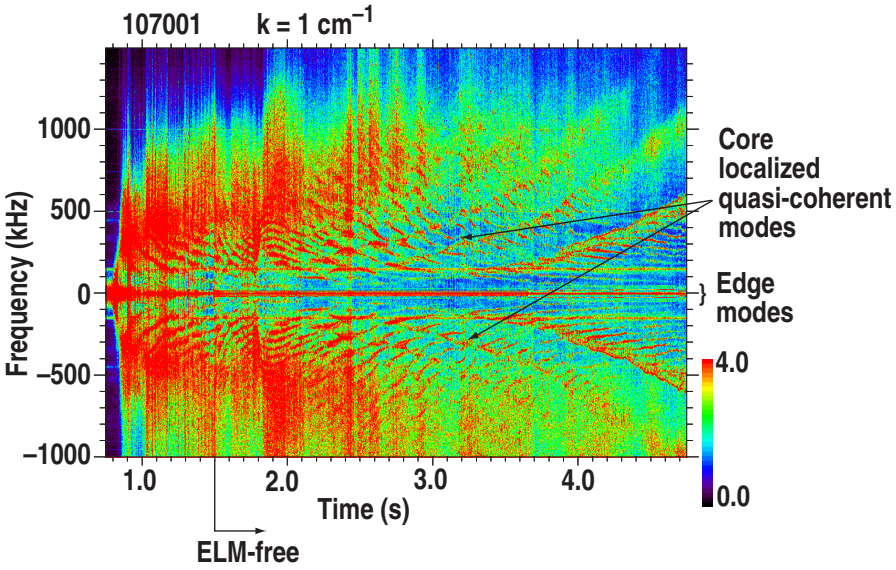

Fig. 5. Contour plot showing amplitude of fluctuations detected by FIR scattering. Suppression of core turbulence is not complete despite the strong ITB during the QDB phase of the discharge which begins at t = 1.5 s (107001).

Despite this significant residual turbulence, the core transport calculated by the TRANSP [20] code in the QDB becomes very small, comparable with that in the L–mode edge ITB discharges, which have more complete turbulence suppression (Fig. 6). Some clues to the nature of these ITBs is provided by simulations of a QDB discharge.

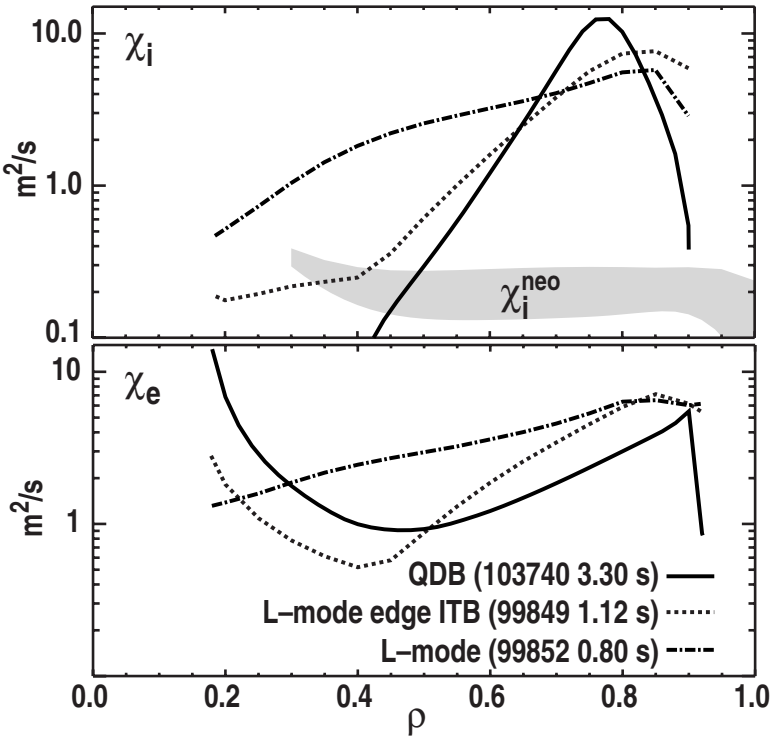

Fig. 6. Thermal diffusivities calculated by TRANSP for QDB (103740), L–mode edge ITB (99849) and standard L–mode (99852) discharges indicate that core transport is similar for QDB and L–mode edge ITB discharges. The region of high transport is visible separating the core and edge barriers.

Linear gyrokinetic stability calculations using the GKS [21,22] code predict a large amplitude kinetic ballooning mode, with $k=0.5\,\mathrm{cm}^{-1}$, appears at $r=0.4$ (Fig. 7). Interestingly, this is the same region where $\omega_{E\times B}$ undergoes a zero-crossing, so that there is no expectation of shear stabilization of this mode. An ideal ballooning mode is predicted at the same location. It is not clear whether this is related to the activity seen on fluctuation diagnostics, although it too appears to be centered near $\rho=0.4$. Outside of this region, comparison of the maximum linear growth rate γ_{max} from the GKS calculation with $|\omega_{E\times B}|$ indicates that the $E\times B$ shear is expected to be sufficient to suppress the turbulence.

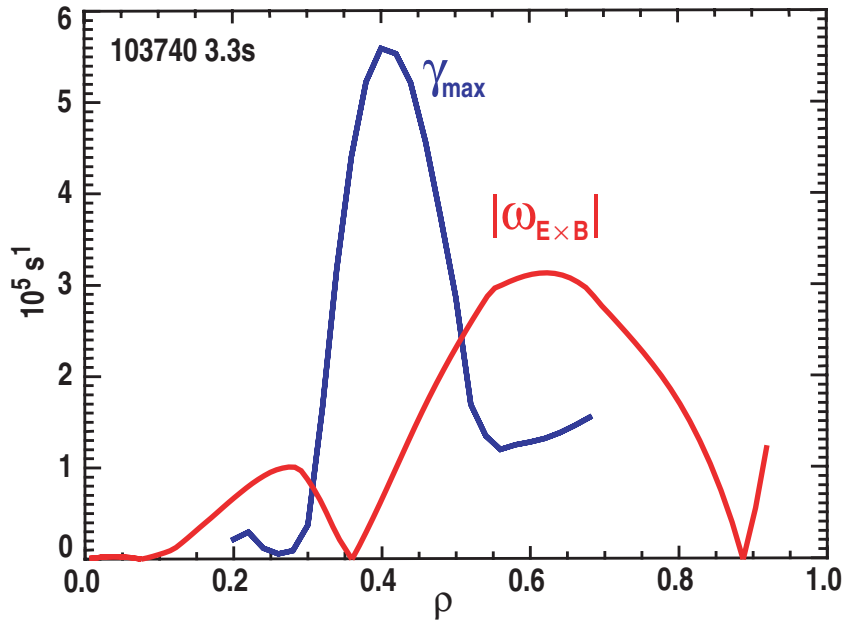

Fig. 7. Comparison of the calculated linear growth rate for drift wave turbulence with the $E \times B$ shearing rate indicates an unstable region, identified as a kinetic ballooning mode, near $\rho \approx 0.4$ (103740 3.3s).

Steady-state simulation of a QDB discharge using the GLF23 gyro-Landau-fluid transport model [23] reproduces the core ion temperature profiles, also with only incomplete suppression of turbulence (Fig. 8). Here, the shearing rate γ_e is very close to the growth rate γ_{max} over a large region of the plasma. This indicates only partial suppression of turbulence, yet the code reproduces the ITB in the ion channel. It also predicts the formation of a similar barrier in the electron channel, which is not reflected in the experimental results.

In the QDB discharges, we have created core barriers with transport characteristics similar to those with complete turbulence suppression, but the turbulence amplitudes remain fairly large. However, the amplitude alone does not determine transport. Reflectometry measurements (Fig. 9) indicate that the turbulence correlation lengths become very small in the core of QDB discharges, indicating a reduction in the step size for transport. In L–mode, the correlation length is generally proportional to a gyroradius. In the QDB, however, this dependence seems to be eliminated, and the correlation length becomes small (but clearly non-zero) and independent of any quantity that varies along the plasma radius. This behavior is replicated by initial efforts at modeling ITG turbulence with the circular geometry UCAN code [24]. Further modeling will be required to verify this result, as the calculation does not yet include all of the pertinent physics.

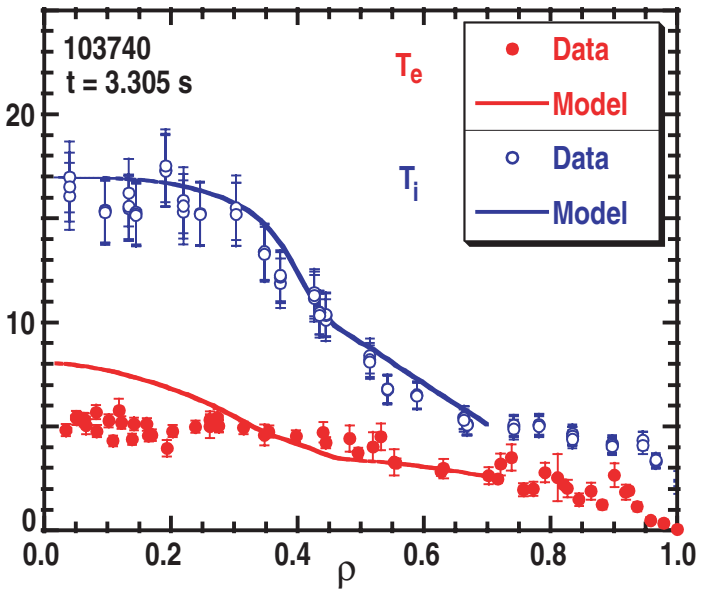

Fig. 8. The ion temperature profile calculated by a steady state simulation using the GLF23 transport mode closely matches the measured profile. However, the electron temperature is not reproduced well (103740).

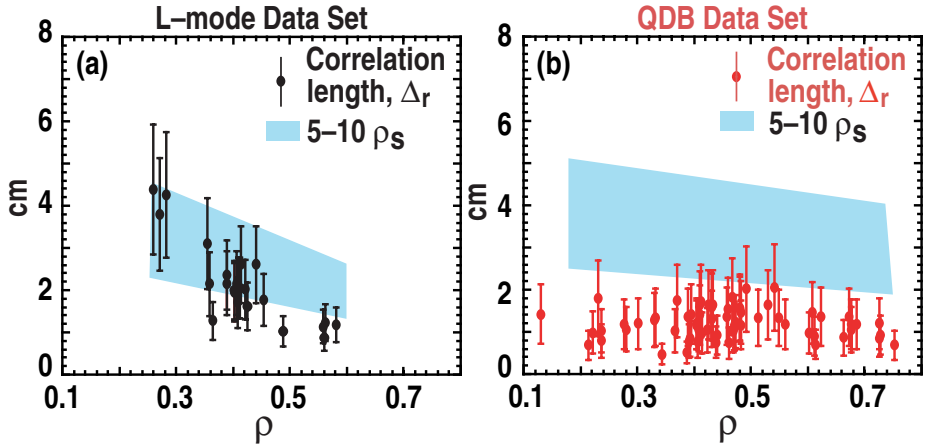

Fig. 9. (a) Turbulence correlation lengths measured by reflectometry in an L–mode discharge vary with the ion gyroradius. (b) In the QDB discharge, they are uniformly small, indicating a reduced step size for turbulence transport.

As mentioned at the beginning of this section, the density profile in the QDB regime is often quite peaked. This has several implications. First the bootstrap current alignment is inadequate for sustainment of the QDB regime without some kind of active current drive (Fig. 10). Fortunately, simulations using the CORSICA [25] transport code predict that the QDB may provide a suitable target for sustainment with electron cyclotron current drive (ECCD; Fig. 11). This indicates that there may be a steady-state solution for the QDB, even though the QDB with counter-NBI has a significant amount of counter current drive from neutral beams (Fig. 10).

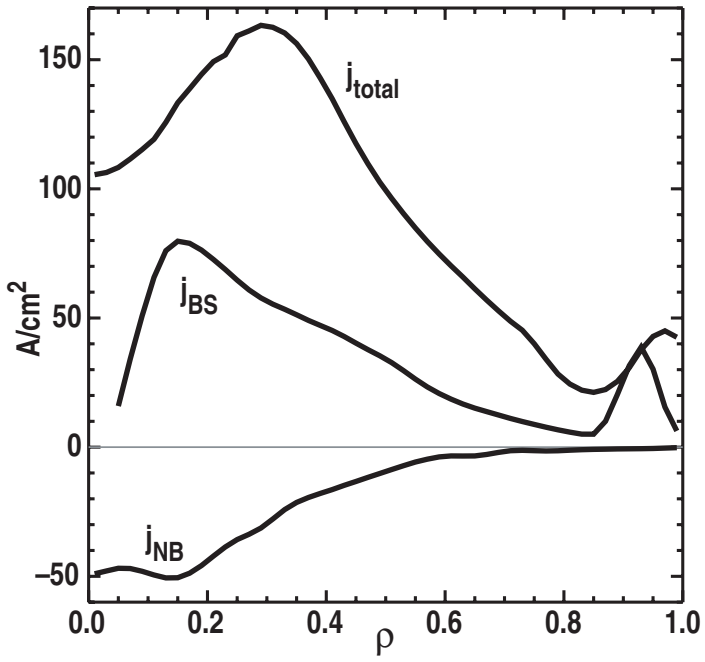

Fig. 10. Current profiles for QDB discharge showing the total current profile along with the calculated bootstrap and neutral beam current drive profiles (103740 3.3 s).

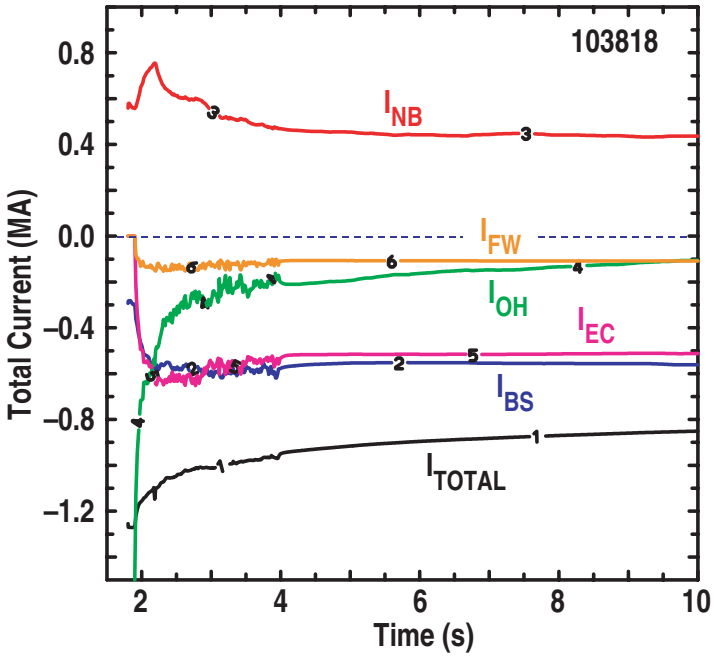

Fig. 11. Calculations using CORSICA predict that ECCD should be able to maintain a steady current profile in a QDB discharge. This simulation includes 3 MW FWCD and 6 MW ECCD. The FW and EC requirements are relaxed if beam ion losses are included (103818).

Production of a QDB discharge without the requirement for counter-NBI would also be very helpful in this regard and will be the subject of future efforts. The core-edge separation should be maintained with balanced NBI as well, since the shearing rate is dominated by the pressure term for both balanced and counter-NBI heated discharges [16]. Whether counter-NBI is a requirement for the edge condition (EHO without ELMs) is still an open question.

The second implication of the peaked density profiles is their impact on impurity confinement. As shown earlier, these discharges can reach a state with steady electron density and radiated power (Fig. 1). However, spectroscopic measurements and MIST [26] modeling indicate that high-Z impurities in non-radiating states continue to increase in QDB discharges.

This is borne out by the results of neoclassical impurity transport modeling using the STRAHL [27,28] code. These calculations predict central accumulation of high-Z impurities as a consequence of the high density peaking $\left[n_e(0)/\langle n_e\rangle \sim 2-3\right]$ [Fig. 1(g)]. At the same time, low-*Z* impurities such as carbon are not predicted to collect in the core.

5. MHD STABILITY

It has long been known that global MHD stability improves as the pressure profile is broadened [29,30]. L–mode edge ITB discharges often exhibit quite low beta limits; this is believed to be a consequence of their relatively peaked pressure profiles (Fig. 12). The stability limit for H–mode discharges is higher since the pressure profile is less peaked.

Analysis of a QDB discharge indicates that it follows a similar trajectory to a typical H–mode discharge in $P(0)/\langle P\rangle$ (pressure profile peakedness)/β_N (normalized beta) space. Access to significantly higher performance by further broadening of the pressure profile in the QDB discharges seems plausible. The peaked pressure profiles in these discharges is largely a consequence of the peaked density profiles.

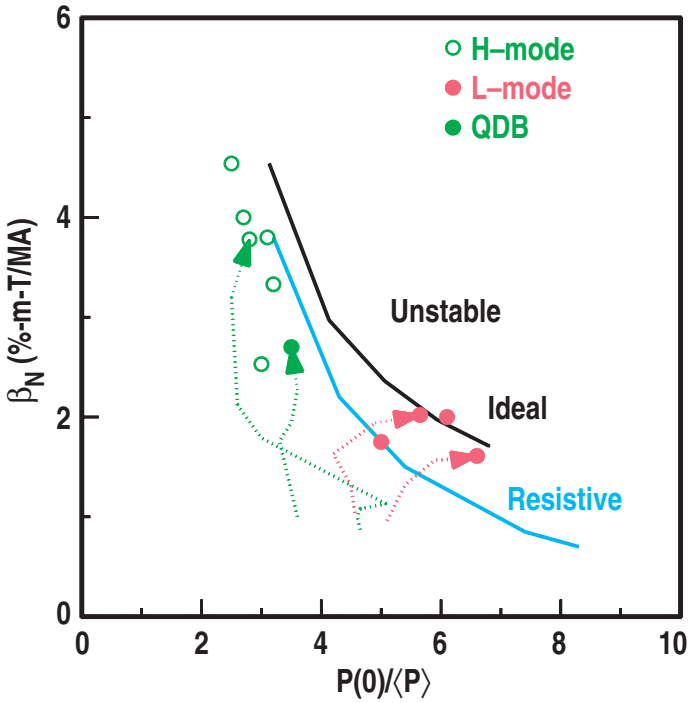

Fig. 12. β_N vs. $P(0)/\langle P\rangle$ trajectories for discharges in L– and H–mode and in the QDB regime. The QDB discharge follows a trajectory similar to standard H–mode. The black curve represents the calculated $n=1$ ideal MHD stability limit and the blue represents the $n=1$ resistive interchange stability limit.

Although detailed studies of the beta limit have not yet been undertaken for the QDB regime, Fig. 12 is representative of the experience with this regime. The highest β_N

achieved in a QDB discharge to date is β_N = 2.9 m–T/MA. Attempts to increase beta by adding additional heating power have in many cases led to disruption; the details of such discharges have not yet been studied.

Another class of instabilities that appear prevalent in the QDB discharges is the Alfvén eigenmodes [31]. Both magnetic and local fluctuation measurements suggest the presence of such activity, indicated by coherent, high frequency signals in many QDB discharges.

In Fig. 13, we compare observations from a pair of similar QDB discharges, but one was operated with a reduced neutral beam injection energy (the heating power was kept nearly fixed by increasing the number of beam sources). In this case, the signature of Alfvén activity in the magnetic measurements is eliminated.

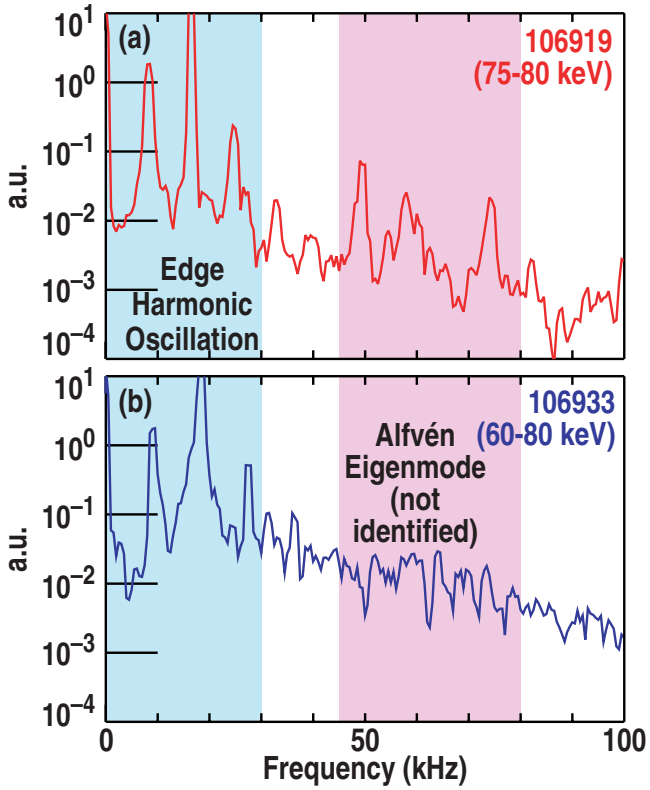

Fig. 13. The power spectrum from $\dot{B}_\theta$ probes indicating EHO and Alfvén mode activity. (a) 106919, 75–80 keV, P_{NBI} = 9 MW, (b) 106933, 60–80 keV, P_{NBI} = 10 MW.

TRANSP analyses in DIII–D often make use of a feature that allows an anomalous beam ion diffusivity to be specified. This feature can effectively mimic the effects of some Alfvén instabilities by artificially redistributing beam ions. In most cases in DIII–D, inclusion of a small anomalous beam ion diffusivity (0.3 m^2/s) is sufficient for the

calculated stored energy and neutron rates to closely match the measured quantities, indicating acceptable reproduction at the effects of the Alfvén eigenmode. In order to match these quantities in many QDB discharges, larger values are needed. In the discharge with reduced beam energy, however, no anomalous beam ion diffusivity is necessary, once again indicating that the Alfvén activity is either eliminated or sharply reduced in this discharge.

The temperature profiles in this pair of discharges are very similar (Fig. 14). Notable differences are seen in the density and rotation behavior. Decreasing the beam energy at fixed power results in increased particle source and beam torque. The former is the cause of the increased peakedness in the density profile. The latter would normally be expected to result in increased rotation; this is not the case, indicating that momentum transport increases in this case. The energy confinement in both cases is similar, indicating that the Alfvén eigenmodes are fairly benign, having little effect on the plasma performance.

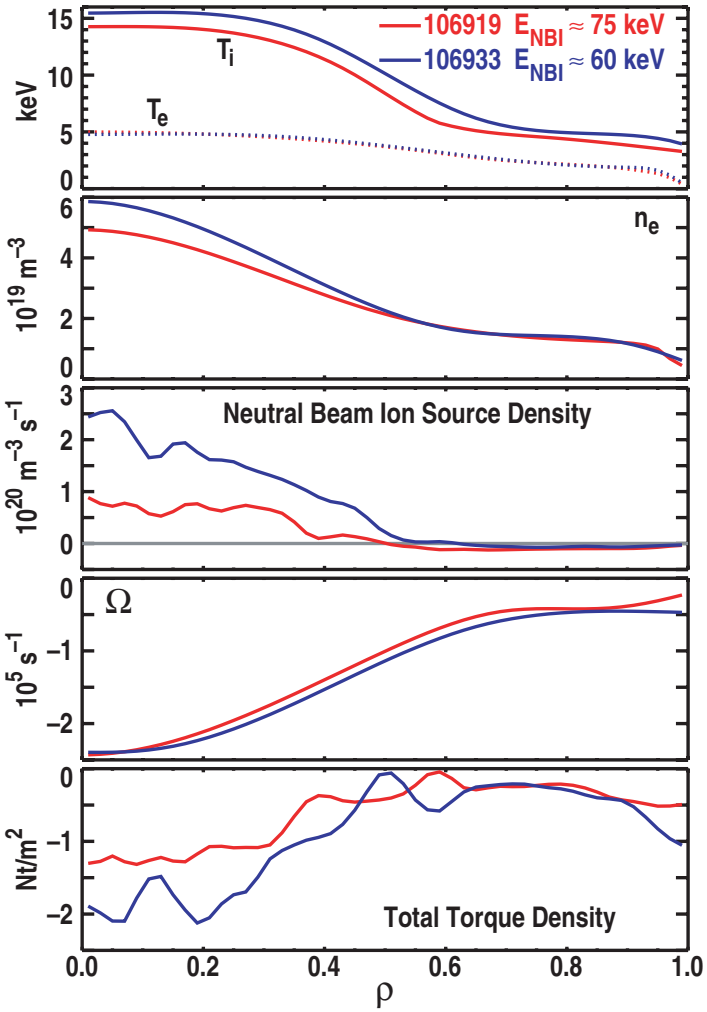

Fig. 14. Kinetic profiles for a pair of QDB discharges operated with different beam energies. P_{NBI} = 9–10 MW.

6. SUMMARY

A new confinement regime, the QDB regime, has been obtained in DIII–D. The QDB regime is characterized by high fusion performance, which is achieved by a combination of an edge and core barrier. The two barriers are maintained separately by a region of low $E \times B$ shear, which arises from a flattening of the E_r profile. The combination is exceptionally stable, and can be sustained for several seconds.

The edge barrier is ELM-free, but with particle transport being modulated by MHD activity. Although the exact nature of the MHD does not appear critical, most of these discharges exhibit the EHO [15]. In some cases, the EHO is replaced by a global MHD mode with a significant component near the edge. Regardless of the nature of the edge MHD, it must not have a core component that is large enough to negatively impact the core barrier.

The core barrier is similar to those seen with L–mode edge ITBs, but with the temperature profiles elevated by the pedestal values, which can be as large as $T_i^{ped} \sim 6$ keV. In contrast with previous experience with ITBs, these form and are sustained with only incomplete suppression of turbulence. Rather, the turbulence correlation lengths, and therefore the transport length scales, become very short.

The core density profiles are quite peaked, even more so than the L–mode edge ITB. This is a consequence of the strong pumping near the edge and the core beam fueling. This results in a narrow bootstrap current profile and enhanced neoclassical impurity retention. Future efforts to optimize the QDB regime will focus on broadening the density profile. Although $\beta_N \approx 2.9$ m–T/MA has been obtained in QDB discharges, broadening the density, and therefore pressure, profile is hoped to also allow access to higher beta.

7. REFERENCES

[1] Greenfield C M et al 1999 *Nucl. Fusion* **39** 1723
[2] Synakowski E J et al 1997 *Phys. Rev. Lett.* **78** 2972
[3] Shirai H et al 1999 *Nucl. Fusion* **39** 1713
[4] Gormezano C et al 1998 *Phys. Rev. Lett.* **80** 5522
[5] Grüber, O et al 1999 *Phys. Rev. Lett.* **83** 1787
[6] Groebner R J 1993 *Phys. Fluids* **B 5** 2343
[7] Lao L L et al 1999 *Bull. Am. Phys. Soc.*. **44** 77
[8] Chan V S et al 1999 *Bull. Am. Phys. Soc.*. **44** 79
[9] Rice B W et al 1999 *Nucl. Fusion* **39** 1855
[10] Greenfield C M et al 1997 *Phys. Plasmas* **4** 1596
[11] Strait E J et al 1997 *Phys. Plasmas* **4** 1783
[12] Greenfield C M et al 2001 *Phys. Rev. Lett.* **86** 4544
[13] Burrell K H et al 2001 *Phys. Plasmas* **8** 2153
[14] Doyle E J et al 2000 Proc. of the 18th IAEA Fusion Energy Conference, Montreal, Canada (International Atomic Energy Agency) published on CD.
[15] Burrell K H et al 2001 "*Quiescent H-mode Plasmas in the DIII-D Tokamak*," presented at this workshop
[16] Greenfield C M et al 2000 *Phys. Plasmas* **7** 1959
[17] Johnson L C et al 2001 Proc. 28th EPS Conference on Controlled Fusion and Plasma Physics, Madeira, Portugal, (European Physical Society) paper P4.008
[18] Hahm T S and Burrell K H 1995 *Phys. Plasmas* **2** 1648
[19] Waltz R E 1998 *Phys. Plasmas* **5** 1784
[20] Hawryluk R J 1980 Proc. of the Course in Physics Close to Thermonuclear Conditions, Varenna, 1979 (Commission of the European Communities, Brussels, 1980), Vol. I, p. 19
[21] Kotschenreuther M 1992 *Bull. Am. Phys. Soc.* **37** 1432
[22] Miller R E et al 1998 *Phys. Plasmas* **5** 973
[23] Waltz R E et al 1997 *Phys. Plasmas* **4** 2482
[24] Sydora R D et al 1996 *Plasma Phys. and Control. Fusion* **38** A281
[25] Casper T A et al 1998 Proc. 25th EPS Conference on Controlled Fusion and Plasma Physics, Prague, Czech Republic (European Physical Society) p. 652
[26] Hulse R A 1983 *Nucl. Technologies/Fusion* **3** 259
[27] Behringer K 1987 JET Joint Undertaking Report JET-R(87)08, Culham, United Kingdom
[28] Peeters A G 2000 *Phys. Plasmas* **7** 268

[29] Lao L L et al 2000 *Phys. Plasmas* **7** 268
[30] Turnbull A D et al 1998 *Nucl. Fusion* **38** 1467
[31] Heidbrink W W et al 1999 *Phys. Plasmas* **6** 1147

8. ACKNOWLEDGMENT

Work supported by U.S. Department of Energy under Contract Nos. DE-AC03-99ER54463, W-7405-ENG-48, DE-AC05-00OR22725, DE-AC02-76CH03073, and Grants DE-FG03-01ER54615, DE-FG03-96ER54373, DE-FG02-92ER54141, and DE-FG03-95ER54294.